SPATIAL AND TEMPORAL PERTURBATIONS VARIABILITY IN TROPICAL AND EXTRATROPICAL SYSTEMS IN SOUTH AMERICA

Adrián Enrique Yuchechen [*]
PEPACG, UCA/CONICET, Buenos Aires, Argentina
Susana Amalia Bischoff
Departamento de Ciencias de la Atmósfera y los Océanos, FCEyN, UBA, Buenos Aires, Argentina
Pablo Osvaldo Canziani
PEPACG, UCA/CONICET, Buenos Aires, Argentina

ABSTRACT

Climate variability at different scales of the atmosphere is a research field that has received a very special interest in recent years. In this work we study the temporal and spatial atmospheric circulation variability, through an analysis of monthly anomalies for the 850 hPa at three South America rawinsonde stations.

In particular, we analyze extreme anomalies in the eastern region of tropical and extratropical South America, and its regional behaviour related to climatic change. Also, a latitude-longitude comparison is presented.

For this study we use rawinsonde data from Argentina (Córdoba and Ezeiza) and the south of Brazil (Galeão) spanning the period January 1973 - October 2005 and covering an area of interest limited by the latitudes 20º S and 40º S. The two former stations represent the extratropical region, while the latter represents the tropics. Geopotential heights obtained from the rawinsondes are the variables used in this analysis.

The methodology used consists in the application of basic statistics parameters, Fourier analysis, and a cluster analysis to classify the atmospheric circulation fields.

1.   AIM

The aim of the present work is to identify circulation patterns associated with 850 hPa monthly mean geopotential height extreme events, and to analyze the possible relation between tropical and extratropical regions.

2.   DATASETS AND METHODOLOGY

This analysis has been based on the Department of Atmospheric Science (College of Engineering) of the University of Wyoming rawinsonde database, which is freely available to researchers. Soundings taken at Galeão (SBGL) (φ=22º48' S, λ=43º15' O), Córdoba (SACO) (φ=31º19' S, λ=64º13' O) and Ezeiza (SAEZ) (φ=34º49' S, λ=58º32' O) were used. Only soundings taken at 12 UTC were used. The dataset covers the period January 1973 – October 2005.

First of all we calculate monthly means for the complete period (i.e., climatic means) for the 850 hPa geopotential height at all three stations (Fig. 1). Once we have the monthly means, we apply a harmonic analysis (Jenkins and Watts, 1968) to them in order to determine the mean annual evolution. The obtained harmonics show that the annual wave dominates at SBGL with 93% of explained variance. At the other two stations the dominant wave is the semiannual one, with 93% of explained variance at SACO, and 92% of explained variance at SAEZ. This could be easily observed by looking at Fig. 1.

---
[*] Corresponding author address: Adrián E. Yuchechen, Programa de Estudios de Procesos Atmosféricos en el Cambio Global (PEPACG), UCA/CONICET, Cap. Gral. Ramón Freire 183, C1426AVC, Buenos Aires, Argentina
e-mail: aey@uca.edu.ar
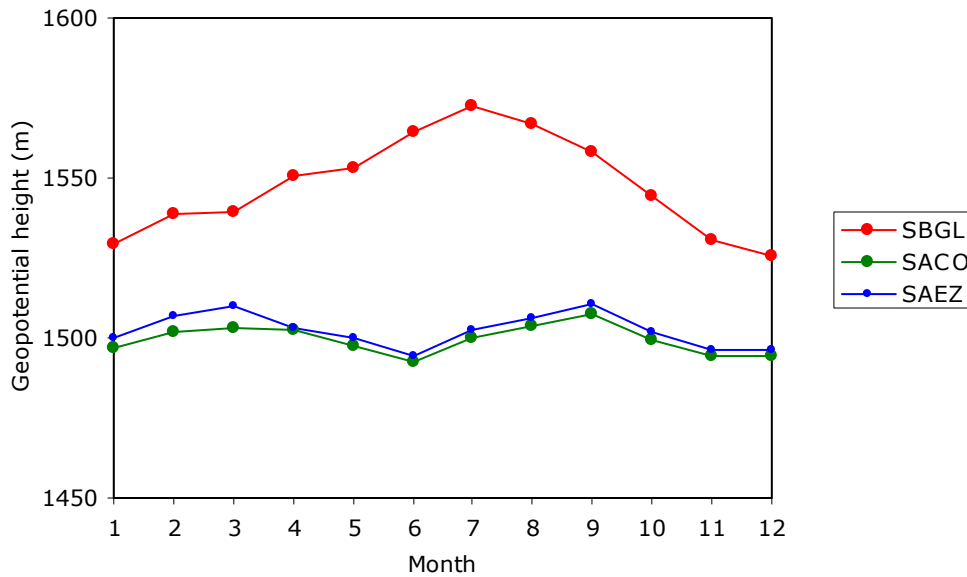
Fig. 1 – 850 hPa climatic geopotential height monthly means

Using the obtained harmonics, we build for each station the mean annual evolution by including all significant harmonics explaining more than 90% of the variance. According to Fig. 1 these basically correspond to the annual one for SBGL and to the semiannual one for the other two stations. We then subtract this from every monthly mean, just to obtain the height monthly mean anomalies for the full period, thus removing the deterministic component included in the raw data. Hence, we obtain the 850 hPa geopotential height anomaly time series that will be studied (Fig. 2). These monthly mean anomalies time series have a missing data maximum at SACO (10%) and a minimum at SAEZ (3% of missing data).
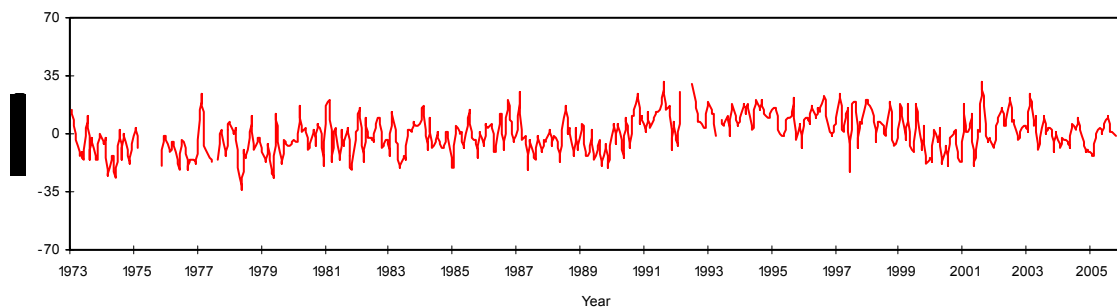
Fig. 2 a) – 850 hPa geopotential height monthly anomalies time series at SBGL
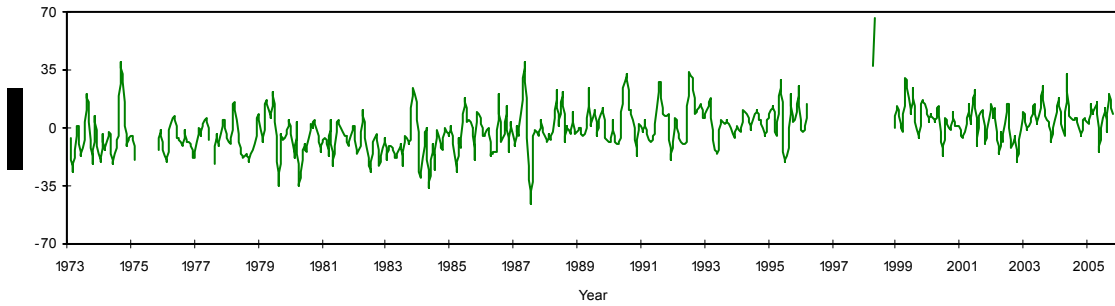
Fig. 2 b) – Same as Fig. 2 a) but for SACO
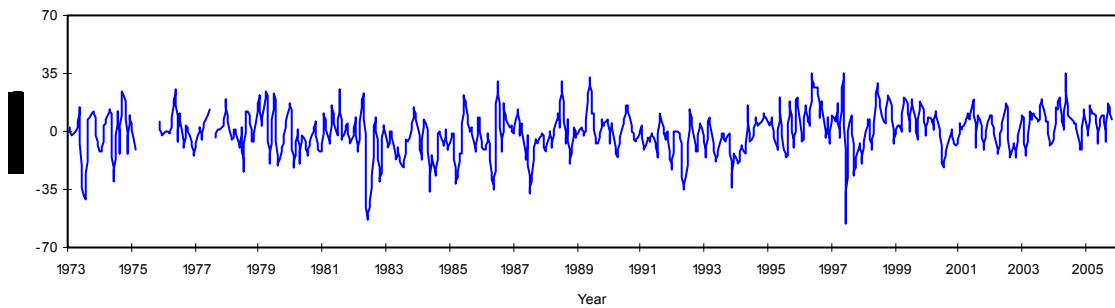
Fig. 2 c) – Same as Fig. 2 a) but for SAEZ

A way to compare the behaviour of the anomalies at each station is to use the empiric distribution function obtained from the sequences of months with equal sign of anomaly. We must keep in mind that the lack of data limits the results. The set of plots in Fig. 3 show the frequency distribution for the sequence of positive and negative anomalies in each case. The maximum number of anomalies with the same sign reaches no more than nineteen consecutive months at all three stations.
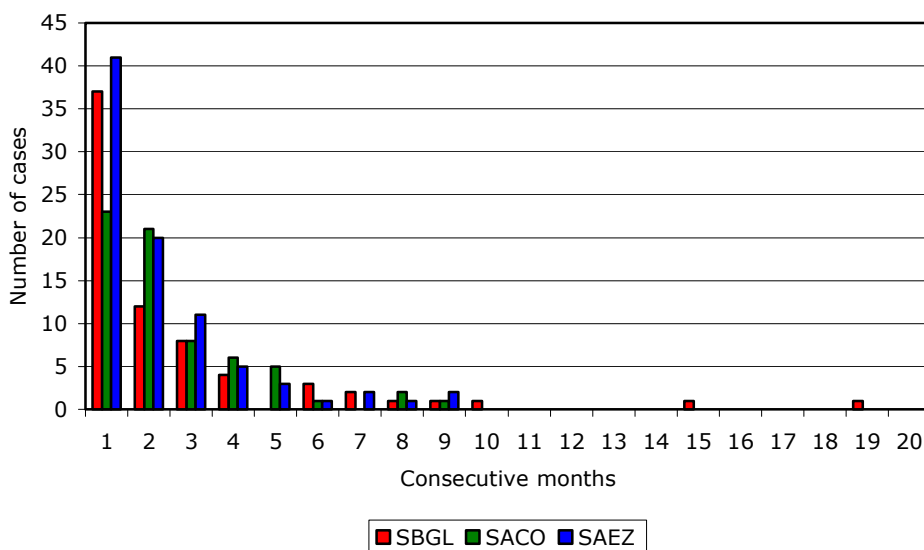
Fig. 3 a) – Frequency distribution for consecutive months with positive values of 850 hPa geopotential height monthly mean anomaly
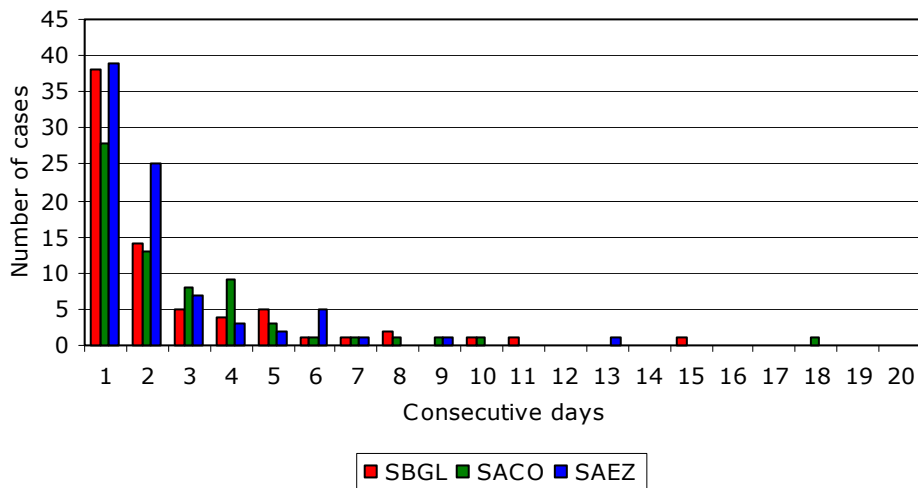
Fig. 3 b) – Same as Fig. 3 a) but for negative anomalies

In all cases the frequency distribution has a decreasing exponential shape whether the anomalies are positive or negative. The decrease from a single month with the anomaly of some sign to two consecutive months with the same anomaly sign is fastest at SBGL. At the extratropical stations this decrease is slowler, meaning that the interannual variability is not as important as in SBGL.

Once we have 850 hPa level monthly mean anomalies for each station, we classify them by a quintile method classification. To deal with extreme events we have to give special attention to the first and the last quintiles. We will study the behaviour of the 500, 300 and 100 hPa levels at all the three stations when an extreme event occurs at the 850 hPa level.

Those months classified as extreme events are used to select the corresponding monthly mean anomalies fields from the NCEP/NCAR reanalysis database[*] (Kalnay *et al.*, 1996). These fields are to be used for the Principal Component Analysis (PCA). Our area of interest is located in latitudes within 10º - 60º S and longitudes within 20º - 120º O. We use the Principal Component Analysis method in mode T, using the correlation matrix as the input (Green et al., 1978;

Richman, 1986; Salles et al., 2001). The fundaments of this methodology can be found in Richman (1986). Each subset is analyzed independently from the others.

3.   RESULTS

3.1   Principal components and vertical structure

Table I shows the explained variances for each of the first five extracted components.

PC	SBGL	SACO	SAEZ
1	28.52	31.58	31.26
2	20.12	21.62	18.68
3	15.73	14.22	12.81
4	11.52	10.41	9.98
5	7.94	6.64	9.18

Table I a) – Explained variances (%) for the first five components of the first quintile

PC	SBGL	SACO	SAEZ
1	29.11	29.52	29.92
2	20.51	24.10	21.81
3	13.25	14.53	15.84
4	10.90	10.43	9.72
5	8.24	7.73	8.50

Table I b) – Same as Table I a) but for the last quintile

---

[*] See http://www.cdc.noaa.gov/Composites/Day/

There are no important changes if we compare the explained variance for each of the first five components along the stations. However, it is important to mention that the first component of the first quintile explains a little more variance in SACO and SAEZ than in SBGL. In other words, the main structure of the field of extreme events anomalies is best explained by the first component at the two extratropical stations. This feature doesn't repeat for the higher order components. As to the last quintile, the first component has a more homogeneous explained variance at all three stations.

The set of plots in Fig. 4 show the first component for the 850 geopotential height monthly mean anomalies included in the first quintil. They also show the 850 hPa monthly mean anomalies field having the maximum correlation found (either maximum or minimum) with the first component, and the monthly mean anomalies fields for the 500, 300 and 100 hPa levels for the same month.
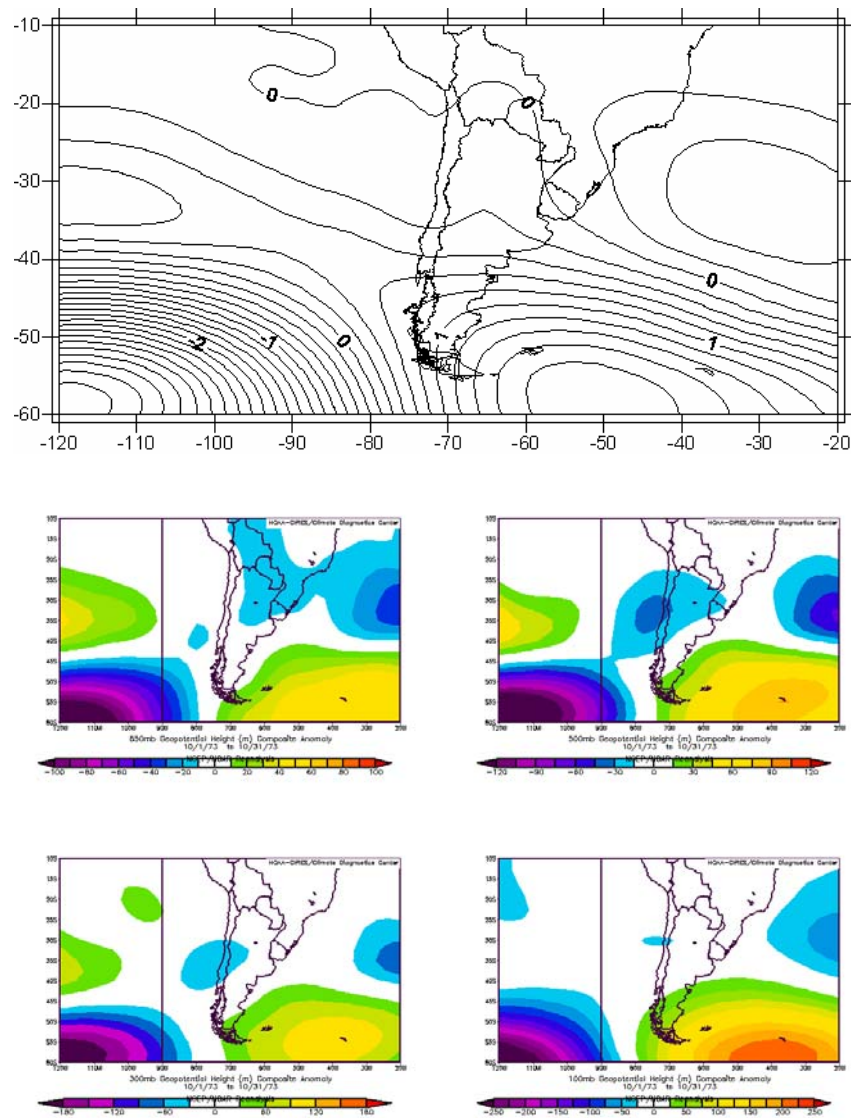
Figure 4 a) – PC1 extracted from the first quintile extreme events for 850 hPa monthly mean geopotential height anomalies at SBGL (top). It also shows the monthly mean geopotential height anomalies fields for October 1973: 850 hPa (centre left), 500 hPa (centre right), 300 hPa (bottom left) and 100 hPa (bottom right). The correlation between the first component and the field of 850 hPa is the maximum found and equal to 0.92

Comparing the first component and the 850 hPa field in Figure 4 a) we see that the first component is related to the presence of four systems at 850 hPa. Two of them represent low pressure systems (one located to the east of the Brazilian coast and the other to the southwest of the Chilean coast) and the other two representing high pressure systems (located to the east of the argentine coast and to the west of the Chilean coast). These systems depict a col (WMO, 1992) over the southern Pacific Ocean, west of the Chilean coast. It can be seen that the same structure also appears in the other fields, with maximum anomalies located al the 100 hPa level.
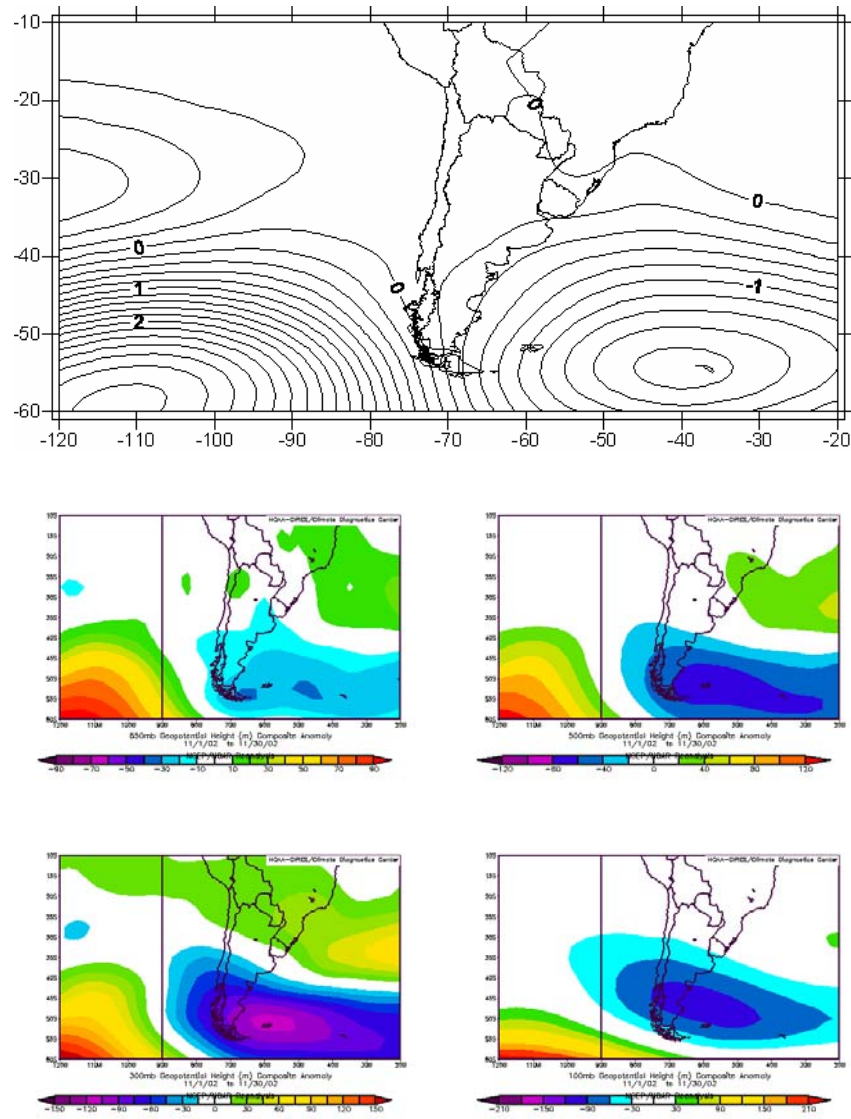
Figure 4 b) – Same a Figure 4 a) but for SACO (November 2002); the correlation between the first component and the field of 850 hPa geopotential anomalies for this date is the maximum found and equal to 0.92

Figure 4 b) represents two opposite systems in both sides of southern South America, south of 35º S: a ridge to the west, over the Pacific Ocean, and a low pressure system to the east, over the Atlantic Ocean. Again, the system structure with height resembles the 850 hPa field, and maximum values of anomalies are reached at the 100 hPa level.
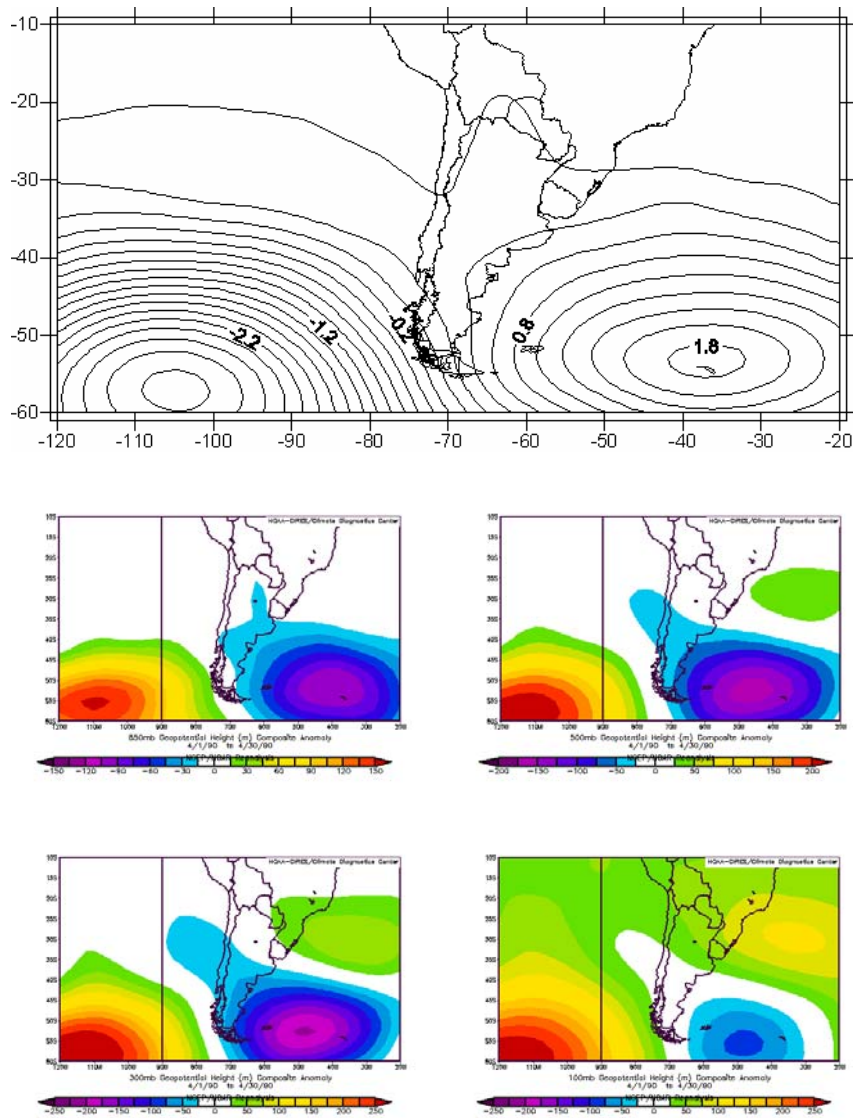
Figure 4 c) – Same a Figure 4 a) but for SAEZ (April 1990); the correlation between the first component and the 850 hPa field is the maximum found and equal to -0.98

In Figure 4 c) we can see that the synoptic situation in southern South America is similar to that shown in Figure 4 b), but with more intense systems. There is present a low pressure system located to the southeast of the Argentine coast, with its center located over the Southern Georgias Islands, and a high pressure system located to the southwest of the Chilean coast, over the southern Pacific Ocean. The vertical structure resembles the 850 hPa field but this time the maximum values of anomalies are reached at both the 300 and 100 hPa level. Moreover, the anomalies present in this set of maps are the strongest ones.

It can be inferred that the circulation field anomalies depicts a zonal high-low pressure dipole south of 35º S for those months associated with the PC1 for both extratropical stations. However, those months associated with the PC1 at SBGL shows the inverted pattern, giving a typical situation of blocking in the southern Atlantic Ocean (Grandoso and Nuñez, 1955; Trenberth and Mo, 1985; Berbery and Nuñez, 1989; Sinclair, 1996; Canziani et al., 2002).

3.2 Interanual variability

This section studies the monthly variability of the extreme circulation patterns. Tables that show the distribution of the best relationship between the 850

hPa level monthly mean anomalies geopotential height and the first five principal components were built to this purpose. The Table II set shows those months associated to each one of the first five principal components. Only extreme events for which the PC *loading* exceeds 0.7 are considered significant. Table II a) shows months included in the last quintile with significant loadings for SBGL. A number from 1 to 5 indicates that that month is significant related to the component. Months marked with an "X" means that that month is not related to any of the first five principal components. Finally, those months with missing data or not classified as an extreme event are left blank.

Year	ENE	FEB	MAR	ABR	MAY	JUN	JUL	AGO	SEP	OCT	NOV	DIC
1973				1	X	X		1		1	X	
1974			X	X	X	1		X		1	4	1
1975											1	
1976		1			1	X			X	X	X	2
1977	3				X	X		X			3	
1978				X	1		3			3		
1979		X		X	2			X				
1980												2
1981			2			X				3	2	
1982			X									
1983	X				1	X	2					
1984												X
1985	X									X		
1986					X							
1987					X		1	X		X		
1988					X					X		
1989		X	X			2			4		X	X
1990					X							
1991												
1992												
1993												
1994												
1995												
1996												
1997						X						
1998												
1999						1					1	X
2000	X				1		1				X	X
2001					X							
2002												
2003											1	
2004											X	
2005	X	X										

Table II a) - Months associated with any of the first five principal components for the first quintile at SBGL

It can be seen from Table II a) that there is a prevalence of highest order components at the beginning of the period for the extreme events included in the first quintile. The opposite situation takes place when we analyze the last quintile (Table II b), where higher order components appear important in the second half of the period. Furthermore, first quintile events are more common before 1990 and last quintile ones are more common after that year.

Year	ENE	FEB	MAR	ABR	MAY	JUN	JUL	AGO	SEP	OCT	NOV	DIC
1973	X						1					
1974												
1975												
1976												
1977		X										
1978									X			
1979						4						
1980			X									
1981	X	2										
1982		X							X			
1983		1										
1984	4	X										
1985							X					
1986						X	X		1			
1987		X										
1988							X					
1989												
1990									X	X		1
1991		X			1	1	1	X	X	1		
1992		1					3	X				
1993	X	2	X					X		X		
1994		2	2	X			1	1	3	1		
1995	X	X						1	X			
1996		X		X		X	X	X	1			
1997		X			X		X	X				X
1998	2	X	1						X			
1999	X	2	X					X	X			
2000												
2001	X			2				5				
2002			1			1						
2003		1		X			X					
2004												
2005							2					

Table II b) – Same a Table II a) but for the last quintile

Thus, the methods applied show an important increase of extreme high events and a decrease of extreme low events since 1990 at SBGL, and SACO shows a similar behaviour. However, SAEZ presents a homogeneous distribution of extreme high and extreme low events for the full period (SACO and SAEZ tables not shown).

3.3 850 hPa geopotential daily anomalies

The aim of this section is to improve the understanding on the behaviour of the 850 hPa geopotential height daily anomalies at SAEZ. For this purpose we include the daily anomaly fields corresponding to the two months with lowest monthly anomaly values in the first quintile (June 1997, June 1982) and the two months with highest monthly anomaly values in the last quintile (May 1996, May 2004). From now on we will call EH (extreme high) to the first set and EL (extreme low) to the last one. We analyze those sets independently from each other by a Principal Component Analysis. Table III show the explained variance for each of the extracted components for both sets.

PC	EL	EH
1	32,32	29,34
2	21,12	24,04
3	16,64	15,89
4	7,23	9,41
5	5,08	5,61

Table III – Explained variances for the first five principal components extracted for the EL and EL set

Fig. 5 shows PC1 for the EH set and the anomalies field for the day with better correlation with it (1 May 1996). The synoptic situation depicted shows a low-high pressure quasi zonal dipole south of 30º S. Hence, PC1 is related to winds blowing from the south at SAEZ.
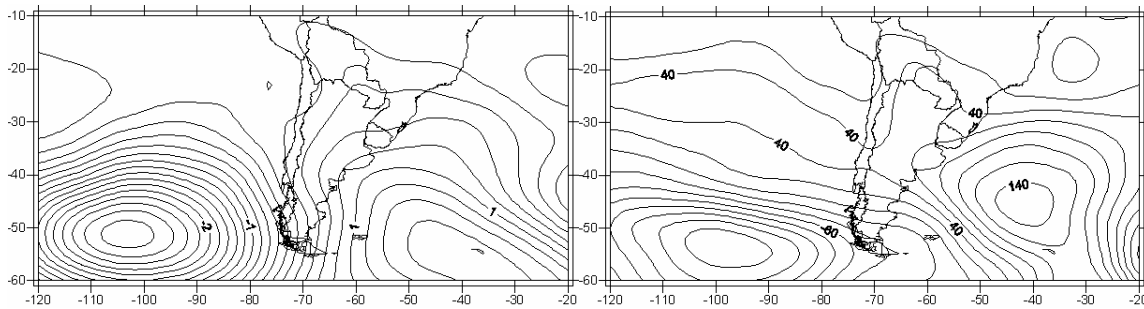
Fig. 5 – PC1 for the EH set (left) and anomalies field for 1 May 1996 (right); the correlation between PC1 and the anomalies field is the maximum found and equal to 0.83

Fig. 6 shows PC2 and the anomalies field having better correlation with it. The synoptic situation shows two low pressure systems located over the oceans and a system of high pressure between them. The circulation pattern depicted gives winds blowing from the west-southwest at SAEZ, a well known regional phenomenon called "Pampero".
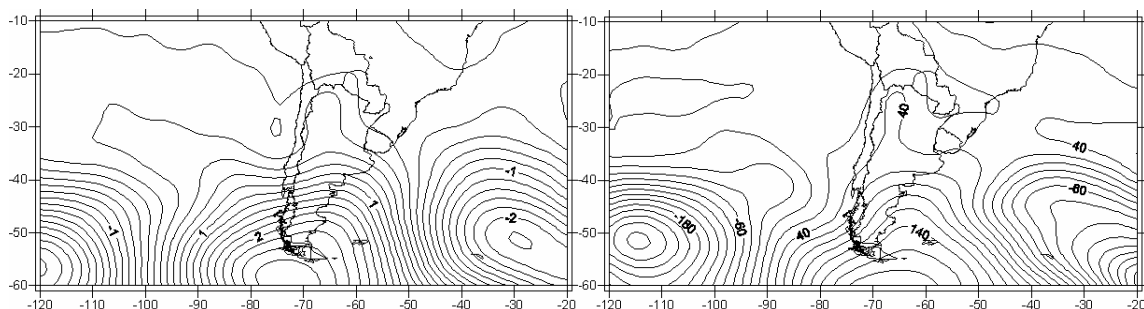
Fig. 6 – PC2 for the EH set (left) and anomalies fields for 30 May 2004 (right); the correlation between PC2 and the anomalies field is the maximum found and equal to 0.83

Fig. 7 shows PC1 for the EL set. As usual, PC1 depicts two systems of opposite sign. The low pressure system is located over the southern Pacific Ocean, whilst the high pressure system is located over the southern Atlantic Ocean. This circulation pattern gives a wind blowing from the southwest at SAEZ, already mentioned as "Pampero".
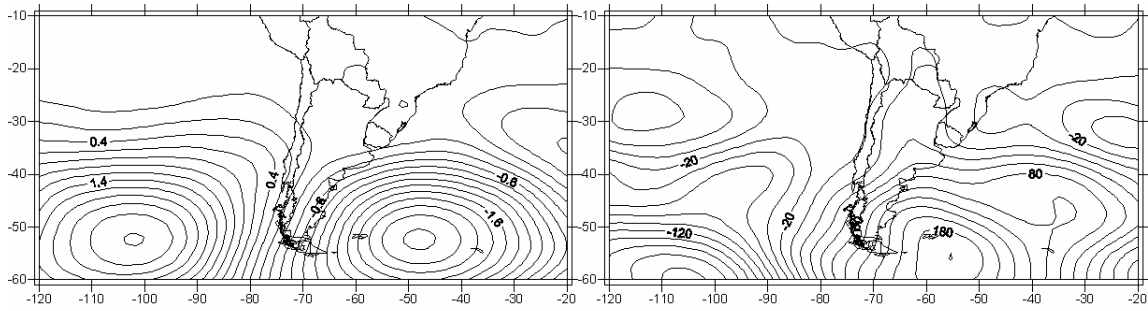
Fig. 7 – PC1 for the EL set (left) and anomalies field for 22 June 1982 (right); the correlation between PC1 and the anomalies field is the maximum found and equal to -0.90

The circulation pattern shown in Fig. 8 corresponds to PC2 for the EL set and depicts a high pressure system over the southern extreme of the continent and two low pressure systems located each one over each ocean. PC2 resembles the way high pressure systems usually crosses the Andes easterly.
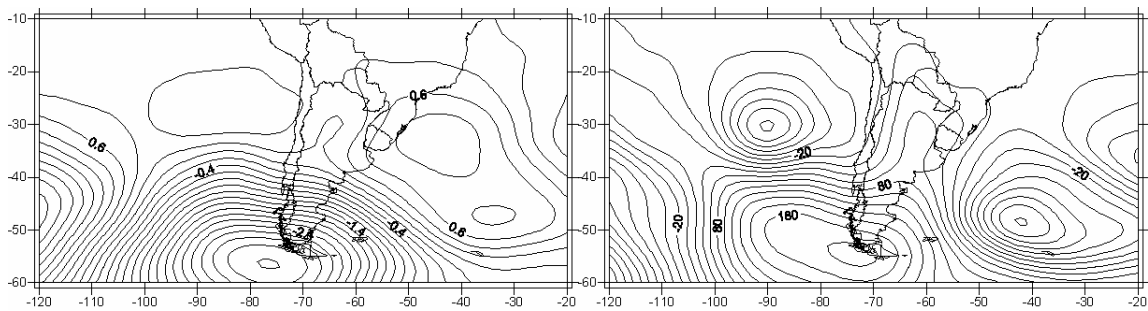
Figure 8 – PC2 for the EL set (left) and anomalies field for 16 June 1982 (right); the correlation between PC2 and the anomalies field is the maximum found and equal to -0.84

4.   CONCLUSIONS

As to the anomalies time series, it can be seen the appearance of a change of sign at SBGL and SACO from 1990 onwards. This phenomenon is not observed at SAEZ. To the scale of analysis of this work, it could be inferred that SBGL and SACO are driven by the same dynamic conditions. This can be associated to variations in the behaviour of the patterns representing each of the months, already analyzed (Tables II a, b). This could be due to the southward displacement of the semi permanent South Atlantic anticyclone (Escobar et al., 2004). The authors will keep on researching about the relation between the change of sign of the anomalies and the displacement of the semi permanent South Atlantic anticyclone.

As to the analysis of the extreme low 850 hPa geopotential height monthly anomalies, PC1s explains no less than 28% of the variance at all three stations. If we compare the PC1s obtained we note that there are present two different regimes: one tropical and one extra tropical. Regionally, to first approximation both regimes are well described by a dipole. When analyzing SBGL, this dipole can be associated with blocking situations at the southern extreme of the continent. Analyzing the extra tropical stations this dipole appears inverted. Moreover, this behaviour repeats with height.

5.   ACKNOWLEDGMENTS

6. REFERENCES

Berbery, E. H. and M. N. Nuñez, 1989: "An observational and Numerical Study of Blocking Episodes near South America", *Journal of Climate,* **2 (12)**, 1352-1361

Canziani, P. O., R. H. Compagnucci, S. A. Bischoff and W. E. Legnani, 2002: A study of impacts of tropospheric synoptic processes on the genesis and evolution of extreme total ozone anomalies over southern South America, *J. Geophys. Res.*, **107 (D24)**, 4741, doi: 10.1029/2001JD000965

Compagnucci, R.H., M. A. Salles and P.O. Canziani, 2001: "The spatial and temporal behaviour of the lower stratospheric temperature over the Southern Hemisphere: the MSU view. Part I: Data, Methodology and Temporal behaviour", *Int. J. of Clim.,* **21**, 4, 419-437

Escobar, G. C. J., I. Camilloni and V. Barros, 2004: Desplazamiento del anticiclón subtropical del Atlántico Sur y su relación con el cambio de vientos sobre el estuario del Río de la Plata, *V Jornadas Nacionales de Ciencias del Mar y XIII Coloquio Argentino de Oceanografía*, Mar del Plata, Argentina, 8-12 December 2004

Grandoso, H. and J. E. Nuñez, 1955: "Análisis de una situación de bloqueo en la parte austral de América del Sur", *Meteoros*, **5 (1-2)**, 35-54

Green, Paul E., 1978: *Analyzing Multivariate Data*, Hinsdale, IL, The Dryden Press, 519 pp.

Jenkins, G. M. and D. G. Watts, 1968: *Spectral Analysis and Its Applications*, Holden-Day, San Francisco, CA, 1968, 275 pp.

Kalnay, E. and Coauthors, 1996: The NCEP/NCAR Reanalysis 40-year Project, *Bull. Amer. Meteor. Soc.*, **77**, 437-471

Richman, M. B., 1986: Rotation of principal components, *Journal of Climatology*, **6**, 3, 293-335

Sinclair, M., 1996: A climatology of anticyclones and blocking for the Southern Hemisphere, *Mon. Wea. Rev.*, **124**, 245-263

Trenberth, K. E and K. C. Mo, 1985: Blocking in the Southern Hemisphere, *Mon. Wea. Rev.*, **113**, 3-21

WMO (World Meteorological Organization), 1992: WMO/OMM/BMO - Nº 182, International Meteorological Vocabulary, Second Edition, Geneva, Switzerland, 784 pp.

---

[*] See http://weather.uwyo.edu/uppeair/sounding.html